

below the dose that induced DLT in three of six patients during the first cycle.

Assessment of Treatment

We used World Health Organization (WHO) criteria to assess the response to treatment of patients who had measurable lesions.²⁰ Measurable lesions were evaluated radiographically. Pleural effusion, ascites, and bone metastases were not considered measurable sites. Patients without measurable lesions were classified as not evaluable.

CA-125 response was defined as a 50% reduction in the CA-125 level below the baseline value that persisted for ≥ 4 weeks. The CA-125 response was assessed and reported separately from the response of patients with measurable disease.²¹ Toxicity was evaluated according to the Japan Clinical Oncology Group Grading system.²²

Pharmacologic Analysis

CPT and carboplatin were infused in 1 arm of each patient, and blood samples for the pharmacokinetic study were taken from each patient's other arm on Day 1 of the first course. Blood samples (1 mL) for pharmacokinetic analysis of CPT-11 were obtained before the chemotherapy; at the end of the CPT-11 infusion; and 5 minutes, 15 minutes, and 30 minutes, 1 hour, 2 hours, 4 hours, 8 hours, and 24 hours after the end of the infusion. The concentrations of CPT-11 and its metabolites (SN-38 and SN-38 glucuronide [SN-38G]) were measured by a modified, reverse-phase, high-performance liquid chromatography method.²³ Blood samples (2 mL) for measurement of carboplatin were obtained before chemotherapy; at the end of the infusion; and 0.5 hours, 1 hour, 2 hours, 4 hours, 6 hours, 10 hours, and 24 hours after the end of the infusion. After immediate centrifugation, the plasma was transferred to an Amicon Centrifree tube (Amicon, Inc., Beverly, MA), and the ultrafiltrates of the plasma were stored at -20°C until measurement of the plasma-free platinum concentration by flameless atomic absorption spectrometry.²⁴ The carboplatin level was calculated based on the platinum/carboplatin molar ratio. The AUC was obtained by the trapezoidal method with extrapolation to infinity using WINNONLIN version 1.1 software (Scientific Consulting, Apex, NC). The biliary index was calculated based on the method described in a previous report.²⁵

In the pharmacodynamic study, we evaluated the correlations between pharmacokinetic parameters and observed hematologic toxicities in the first course. Hematologic toxicity was calculated according to the following formula: percentage decrease = $100 \times (\text{count before treatment} - \text{nadir count}) / (\text{count be-}$

TABLE 1
Patient Characteristics

Characteristic	No. of patients
No. of patients entered	19
Median age in yrs (range)	58 (40-63)
Performance status	
0	6
1	13
Histology	
Serous	15
Mucinous	1
Endometrioid	1
Clear cell	1
Unclassified	1
No. of previous regimens	
1	10
2	6
3	2
4	1
Platinum-free interval	
< 3 mos	10
3-6 mos	3
≥ 6 mos	6
Disease sites	
Pelvic tumor	7
Liver metastasis	3
Lymph node metastasis	3
Ascites	5
Pleural effusion	3
Other	2
Median 24-hr creatinine clearance mL/min (range)	65.9 (16.9-98.8)

fore treatment), and it was related to the AUC according to a sigmoid E_{max} model as follows: Effect (%) = $100 \times E_{\text{max}}(\text{AUC})^{\kappa} / (\text{AUC}_{50})^{\kappa} + \text{AUC}^{\kappa}$. Nonlinear least-squares regression performed with WINNONLIN was used to estimate the AUC that produce 50% of the maximum effect (AUC_{50}) and the sigmoidicity coefficient (κ).

To evaluate for adjustment serum creatinine by adding 0.2 mg/dL,¹⁰ we compared the observed carboplatin clearance with carboplatin clearance calculated with the Chatelut formula using PAP methods with or without the adjustment model. The accuracy of the estimate was measured by calculating the mean predictive error (MPE) and the root mean square error (RMSE).²⁶

RESULTS

Patient Characteristics

In total, 19 patients were enrolled on this trial between August 1996 and July 1999, and all patients previously has received platinum-containing chemotherapy. The patient characteristics are listed in Table 1. Their median age was 58 years (range, 40-63 yrs), and the performance status was 0 in 6 patients and 1 in 13

TABLE 2
Dose-Escalation Schedule and Actual Doses Given to Patients

Level	Dose		No. of patients	Total no. of courses	CPT-11 dose intensity (mg/m ² /wk) delivered/projected	CPT-11 percentage dose delivered ^a
	CBDCA (AUC)	CPT-11 (mg/m ²)				
1	4	50	3	7	30/38	81
2	4	60	3	8	26/45	64
3	5	50	3	7	29/38	80
4	5	60	5	23	25/45	60
5	6	50	5	25	21/38	58

CBDCA: the observed area under the concentration curve (AUC) for carboplatin; CPT-11: irinotecan.

^a Actually delivered CPT-11 dose as a percentage of the planned dose.

TABLE 3
Major Toxicities Stratified by Dose Levels (70 courses)

Level	Toxicity grade															
	Leukopenia		Neutropenia		Anemia		Platelets		Nausea/emesis				Diarrhea			
	3	4	3	4	3	4	3	4	1	2	3	4	1	2	3	4
1	0	0	1	0	1	0	0	0	2	1	0	0	0	0	0	0
2	0	0	0	0	1	0	0	0	2	0	0	0	0	0	0	0
3	0	0	1	0	0	0	0	0	1	1	0	0	0	0	0	0
4	1	0	0	1	3	0	4	0	0	2	0	0	0	1	0	0
5	1	1	2	2 ^a	2	0	1	3	2	1	1	0	2	1	0	0

Platelets: thrombocytopenia.

^a Two patients experienced Grade 3 febrile neutropenia.

patients. Nine patients had received one or more chemotherapy regimens before this study. In total, 70 courses of the regimen used in this study were administered through 5 dose levels, and all patients were assessable for toxicity (Table 2). The median number of courses was 4 (range, 1–7 courses). One-half of the patients (58.2%) in this study actually received CPT-11 on Day 8, but only 31.3% of patients received CPT-11 on Day 15. CPT-11 was withdrawn on Day 8 or Day 15 on 72 occasions, because of thrombocytopenia in 49% of episodes and because of leukopenia in 31% of episodes. However, on 9 occasions, the thrombocyte count was $> 75,000/\mu\text{L}$; and, on 17 occasions, the leukocyte count was $> 2000/\mu\text{L}$. Dose intensity and the percentage of the CPT-11 dose administered that was delivered at each dose level are shown in Table 2.

Recommended Dose Level

None of the 3 patients at Dose Levels 1, 2, 3, and 4 experienced DLTs. Because 1 of the 3 patients at Dose Level 5 experienced DLT (neutropenia and thrombocytopenia), an additional 3 patients were enrolled. Two of those patients developed DLT (neutropenia

and thrombocytopenia); therefore, it was concluded that Dose Level 4 was the MTD and the recommended dose.

Toxicity

Leukopenia and neutropenia were the DLTs associated with this combination chemotherapy. Major toxicities stratified by dose levels are shown in Table 3. At Dose Level 5, 2 patients required platelet infusion and developed febrile neutropenia that required intravenous antibiotics. No anemia that required blood transfusion was observed in any treatment cycle at any level. Gastrointestinal toxicities, such as nausea, emesis, diarrhea, and appetite loss, were prominent. CPT-11 caused diarrhea, but it was mild (Grade 1–2). No treatment-related deaths occurred in the current study.

Responses

Ten patients had measurable lesions, and they were assessed for responses according to WHO criteria (2 patients at Dose Level 1, 2 patients at Dose Level 2, 1 patient at Dose Level 3, 3 patients at Dose Level 4, and

TABLE 4
Objective Response and CA-125 Response

Level	No. of patients	Response				No. of CA-125 responses ^a
		PR	NC	PD	NE	
1	3	0	2	0	1	1
2	3	0	2	0	1	0
3	3	0	0	1	2	0
4	5	3	0	0	2	2
5	5	2	1	0	2	3

PR: partial response; NC: no change; PD: progressive disease; NE: not evaluable.

^a The number of CA-125 responses means number of patients who achieved a 50% reduction in CA-125 level compared with the baseline level, which that must have persisted for ≥ 4 weeks.

3 patients at Dose Level 5). An objective response was observed in 5 patients: a partial response was seen at Dose Level 4 in 3 patients, and a partial response was seen at Dose Level 5 in 2 patients. The platinum-free interval was < 3 months in 2 of the 3 patients who achieved a partial response at Dose Level 4. CA-125 responses were observed in 6 patients (Table 4). The median time to disease progression in this study was 6.1 months (range, 0.93–19.4 mos), and the median survival was 16.2 months (range, 2.5–51.9 mos).

Pharmacologic Study of CPT-11 and CBDCA

The pharmacokinetic study was performed in only 13 patients, because the other 6 patients refused blood sampling for the pharmacokinetic analysis. A summary of the pharmacokinetic parameters of CPT-11, SN-38, and SN-38G is shown in Table 5. The concentrations of CPT-11 and SN-38 versus the time curve at each dose are shown in Figures 1 and 2, respectively. The metabolic ratios of SN-38 and the biliary indexes calculated as the AUC of CPT-11 and the AUC of SN-38/AUC of SN-38G²⁵ were similar at both dose levels.

A summary of the pharmacokinetic parameters of carboplatin is shown in Table 5. The measured AUCs of carboplatin were higher than the estimated AUCs (Fig. 3). The observed carboplatin clearance and the carboplatin clearance calculated using the Chatelut formula were 74.1 ± 24.6 mL/minute (range, 31.8–120.0 mL/min) and 93.7 ± 29.2 mL/minute (range 37.0–138.9 mL/min), respectively. The accuracy of the estimation evaluated on the basis of the MPE and the RMSE was 22.8% and 31.3%, respectively, using the Chatelut formula without the adjustment model and -1.1% and 17% , respectively, on the basis of calculations with the adjustment model (Fig. 4).

The pharmacodynamic analysis was undertaken to evaluate the correlations between pharmacokinetic

parameters and hematologic toxicity in the first course. The correlation between the SN-38 AUC and the percentage decrease in neutrophil count is shown in Figure 5 ($r = 0.292$), and the AUC₅₀ of SN-38 was 36.0 ng/hour/mL, with κ estimated at 0.38. The correlation between the carboplatin AUC and the percentage decrease in thrombocyte is shown in Figure 6 ($r = 0.514$), and the AUC₅₀ of carboplatin was 2.76 mg · min/mL, with κ estimated at 2.80.

DISCUSSION

Based on the results of the current study, the combination of CPT-11 and carboplatin was feasible for patients who previously received platinum-containing chemotherapy, and it was concluded that the recommended dose for the Phase II study in patients with advanced ovarian carcinoma was CPT-11 60 mg/m² on Days 1, 8, and 15 combined with carboplatin AUC 5 on Day 1. To our knowledge, this is the first report of combination therapy with carboplatin and CPT-11 in patients with ovarian carcinoma.

In Phase I trials in previously untreated patients with lung carcinoma, the recommended dose of this regimen was CPT-11 50 mg/m² on Days 1, 8, and 15 and carboplatin AUC 5 mg/mL · minute on Day 1, and the DLTs were neutropenia, thrombocytopenia, and diarrhea.^{27,28} Although the recommended CPT-11 dose in the current study was higher than in those studies, the main DLTs were neutropenia and thrombocytopenia, as expected, and no severe nonhematologic toxicities, such as diarrhea, were observed. We believe that the reasons for this may be that the dose intensity of CPT-11 (mg/m² per week) and the percentage of the dose delivered in our study were lower than in the other studies. The difference of the dose intensity is attributable to the fact that our criteria for administration on Days 8 and 15 were stricter than those used in the previous studies^{17,27,28} and to the difference in the number of patients in a previously untreated or heavily treated setting.

Although the sequence of administration of CPT-11 and carboplatin in the current study was different from the sequence used in the patients with lung carcinoma, the pharmacokinetic parameters of CPT-11 and SN-38 were almost the same as those in the patients with lung carcinoma who were treated with CPT-11 (50 mg/m² on Days 1, 8, and 15) followed by a fixed dose of carboplatin (300 mg/m² on Day 1).²⁸ The sequence of the drug administration in a previous study did not affect the pharmacodynamics or kinetics in the combination of CPT-11 and cisplatin.²⁹ Therefore, the drug sequence administration may have no major influence on the pharmacokinetic parameters in the combination of CPT-11 and carboplatin.

TABLE 5
Summary of Pharmacokinetic Parameters^a

Pharmacokinetic parameter	No. of patients	C _{max}	AUC ^{0-∞}	CL	T _{1/2}	Biliary index ^b
CPT-11		μg/mL	μg·hr/ml	L/m ² hr	Hr	
50 mg/m ²	8	0.69 ± 0.06	3.32 ± 0.25	13.21 ± 1.32	8.03 ± 0.75	—
60 mg/m ²	5	1.14 ± 0.10	4.79 ± 0.44	13.00 ± 1.32	8.35 ± 1.05	—
SN-38		ng/mL	ng·hr/ml		Hr	
50 mg/m ²	8	22.86 ± 2.6	225.6 ± 40.3	—	10.51 ± 1.98	—
60 mg/m ²	5	28.27 ± 4.5	283.9 ± 62.7	—	11.67 ± 2.41	—
SN-38G		ng/mL	ng·hr/ml		Hr	ng·hr/ml
50 mg/m ²	8	29.8 ± 3.1	464.7 ± 70.4	—	12.06 ± 1.50	1692.8 ± 843.7
60 mg/m ²	5	45.6 ± 12.5	1040.2 ± 416.8	—	16.05 ± 1.41	1652.2 ± 511.4
CBDCA		mg/mL	mg·min/ml	mL/min	Hr	
AUC 4	6	13.97 ± 4.1	4.95 ± 0.99	77.7 ± 27.53	4.25 ± 0.74	—
AUC 5	4	16.4 ± 3.3	5.59 ± 0.48	77.99 ± 30.73	4.17 ± 1.23	—
AUC 6	3	21.7 ± 2.5	7.94 ± 1.88	80.69 ± 24.83	4.18 ± 0.37	—

C_{max}: maximum plasma concentrations; AUC: area under the concentration curve; CL: clearance; T_{1/2}: elimination half-life; CPT-11: irinotecan; SN-38: 7-ethyl-10-hydroxycamptothecin; SN38G: SN-38-glucuronide; CBDCA: the observed AUC of carboplatin.

^a Data shown are the mean ± standard deviation in 13 patients.

^b "Biliary index (ng·hr/ml)" was calculated as AUC_{CPT-11} × AUC_{SN-38}/AUC_{SN-38G}.

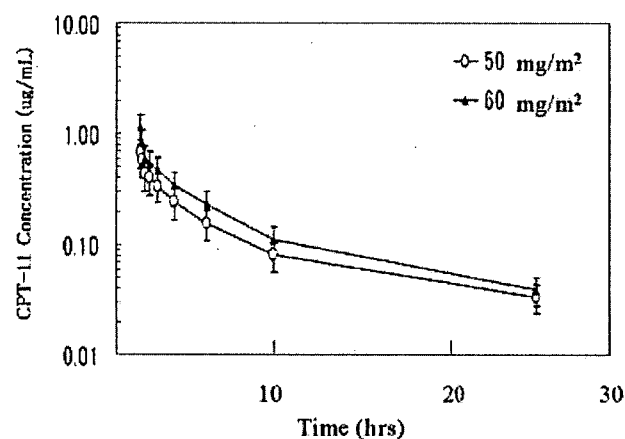


FIGURE 1. The concentrations of irinotecan (CPT-11) versus the time curve are illustrated for patients who received doses of 50 mg/m² and 60 mg/m² (*n* = 13 patients).

Although we used the Chatelut formula in the current study, several formulas are available to calculate the dose of carboplatin. The Calvert formula requires measurement of the glomerular filtration rate with a radioisotope, but creatinine clearance rates estimated by the Cockcroft-Gault or Jelliffe formula or actually measured, 24-hour creatinine clearance have been used widely instead. Several studies have compared the performance of the Chatelut formula and the Calvert formula by using several methods,¹⁴⁻¹⁶ but the performance of each formula remains a matter of controversy, because previous studies have reported differences according to race, gender, method of cal-

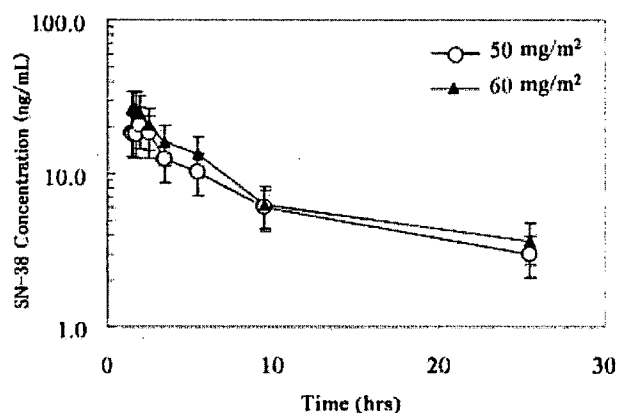


FIGURE 2. The concentrations of SN-38 versus the time curve are illustrated for patients who received in doses of 50 mg/m² and 60 mg/m² (*n* = 13 patients).

culating creatinine clearance, and unknown pharmacokinetic interactions between drugs in combination.¹²⁻¹⁷ Fukuda et al. reported that a Phase I study of CPT-11 and carboplatin in 11 previously untreated Japanese patients with solid malignancies showed a significant correlation between measured carboplatin clearance and carboplatin clearance estimated by the Chatelut formula, and those authors recommended using the formula.¹⁸ However, several clinical pharmacologic studies have shown that carboplatin clearance calculated by the Chatelut formula was higher than measured clearance and clearance calculated by the Calvert formula.¹²⁻¹⁴ Furthermore, it has been reported that the adjusted serum creatinine value is

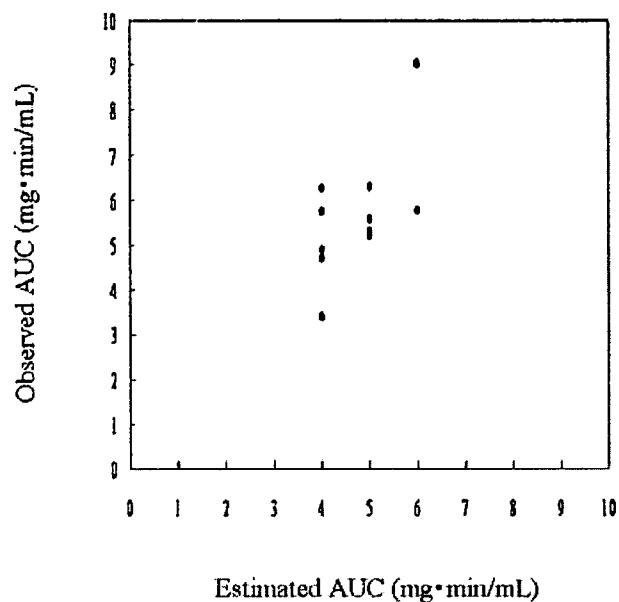


FIGURE 3. This chart illustrates the correlation between the observed area under the plasma concentration-versus-time curve (AUCs) of carboplatin (CBDCA) and the estimated AUC.

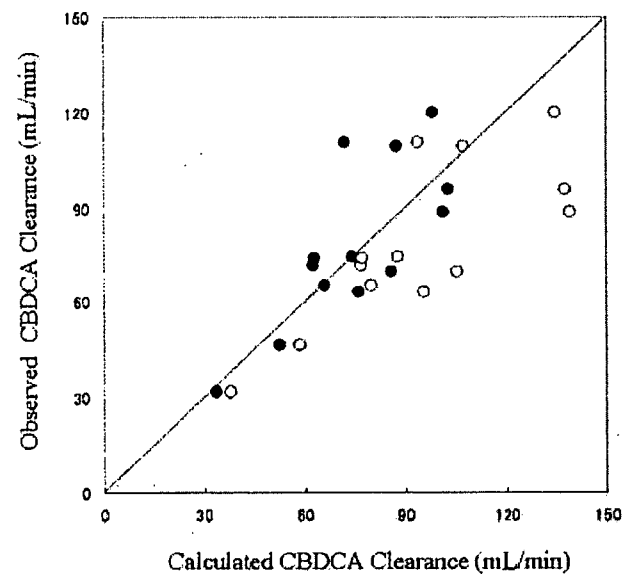


FIGURE 4. This chart illustrates the correlation between observed carboplatin (CBDCA) clearance and CBDCA clearance calculated with the Chatelut formula (open circles) and with the Chatelut formula adjusted for serum creatinine (solid circle) (see Dooley et al., 2002¹⁷). The line of identity (solid line) is shown. The bias and precision of each formula are expressed by the mean prediction error and the root mean square error (see Kaneda et al., 1990²⁴).

appropriate for calculating the proper carboplatin clearance in Japanese patients.¹⁸ Similar to previous reports, our study showed that the calculated carbo-

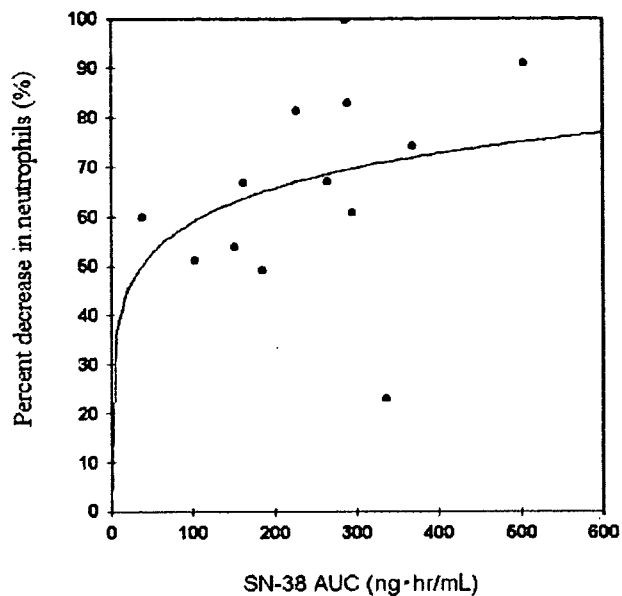


FIGURE 5. This chart illustrates the correlation between the SN-38 area under the plasma concentration-versus-time curve (AUC) and the percentage decrease in neutrophil count in Course 1 based on the sigmoid E_{max} model.

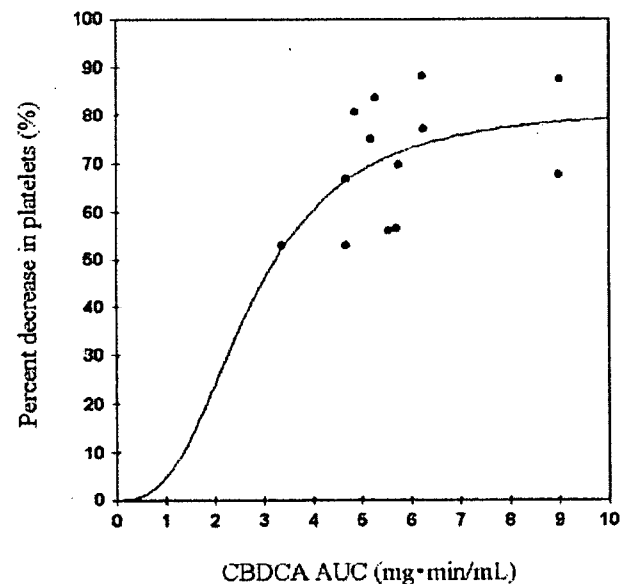


FIGURE 6. This chart illustrates the correlation between the carboplatin (CBDCA) area under the plasma concentration-versus-time curve (AUC) and the percentage decrease in platelet count in Course 1 based on the sigmoid E_{max} model.

platin clearance values were higher than the measured values, and the accuracy of estimation by using the Chatelut formula improved when adjusted serum creatinine values were used.

In recent years, it has been demonstrated that paclitaxel is highly effective for ovarian carcinoma, and paclitaxel plus platinum combination chemotherapy now is accepted widely as a standard regimen for the first-line treatment for advanced ovarian carcinoma.^{1,2} CPT-11 is a topoisomerase I inhibitor that has unique antitumor action. In a Phase II trial, CPT-11 and cisplatin combination chemotherapy yielded a high response rate of 76% in previously untreated patients with advanced ovarian carcinoma.³⁰ CPT-11 and cisplatin also yielded an overall response rate of 40% in patients who were treated previously with platinum-containing chemotherapy and a response rate of 30% in platinum-resistant patients.³¹ Kigawa et al. reported a high response rate (60%) to second-line CPT-11 and cisplatin combination chemotherapy among patients who were treated previously cisplatin, and there was no difference in the proportion of patients who had platinum-sensitive or platinum-resistant tumors between responders and nonresponders.³² Although the current study was performed in a Phase I trial setting, it is noteworthy that half of the patients with measurable lesions achieved responses. A previous study reported that the CPT-11 response rate was 17%, even among patients with platinum-resistant tumors.⁷ Thus, our regimen may be effective both in patients with platinum-sensitive disease and in patients with platinum-resistant disease who previously received paclitaxel plus platinum combination chemotherapy.

In conclusion, the recommended doses of CPT-11 and carboplatin in combination are 60 mg/m² and an AUC of 5 mg/mL · minute according to the Chatelut formula, respectively, and this regimen may be effective in patients with ovarian carcinoma who previously received platinum-containing chemotherapy. The results of the pharmacologic analysis in this study suggest that the carboplatin clearance rates calculated with the Chatelut formula are higher than the actually measured carboplatin clearance and that adjustment for serum creatinine may be useful in calculating the proper dose.

REFERENCES

- McGuire WP, Hoskins WJ, Brady MF, et al. Cyclophosphamide and cisplatin compared with paclitaxel and cisplatin in patients with Stage III and IV ovarian cancer. *N Engl J Med*. 1996;334:1-6.
- Ozols RF, Bundy BN, Greer BE, et al. Phase III trial of carboplatin and paclitaxel compared with cisplatin and paclitaxel in patients with optimally resected Stage III ovarian cancer: a Gynecologic Oncology Group study. *J Clin Oncol*. 2003;21:3194-3200.
- Misawa T, Kikkawa F, Maeda O, et al. Establishment and characterization of acquired resistance to platinum anticancer drugs in human ovarian carcinoma cells. *Jpn J Cancer Res*. 1995;86:88-94.
- Kano Y, Akutsu M, Suzuki K, Yoshida M. Effects of carboplatin in combination with other anticancer agents on human leukemia cell lines. *Leukemia Res*. 1993;17:113-119.
- Kano Y, Suzuki K, Akutsu M, et al. Effects of CPT-11 in combination with other anticancer agents in culture. *Int J Cancer*. 1992;50:604-610.
- Bodurka DC, Levenback C, Wolf JK, et al. Phase II trial of irinotecan in patient with metastatic epithelial ovarian cancer or peritoneal cancer. *J Clin Oncol*. 2003;21:291-297.
- Evans BD, Raju KS, Calvert AH, Harland SJ, Wiltshaw E. Phase II study of JM8, a new platinum analog, in advanced ovarian carcinoma. *Cancer Treat Rep*. 1983;67:997-1000.
- Leyvraz S, Ohnuma T, Lassus M, Holland JF. Phase I study of carboplatin in patients with advanced cancer, intermittent intravenous bolus, and 24-hour infusion. *J Clin Oncol*. 1985;3:1385-1392.
- Jordrell DI, Egorin MJ, Canetta RM, et al. Relationships between carboplatin exposure and tumor response and toxicity in patients with ovarian cancer. *J Clin Oncol*. 1992;10:520-528.
- Calvert AH, Harland SJ, Newell DR, et al. Early clinical studies with cisdiammine-1,1-cyclobutane dicarboxylate platinum II. *Cancer Chemother Pharmacol*. 1982;9:140-147.
- Chatelut E, Canal P, Brunner V, et al. Prediction of carboplatin clearance from standard morphological and biological patient characteristics. *J Natl Cancer Inst*. 1995;87:573-580.
- Fujiwara Y, Takahashi T, Yamakido M, Ohune T, Tsuya T, Egorin MJ. Re: prediction of carboplatin clearance from standard morphological and biological patients characteristics. *J Natl Cancer Inst*. 1997;89:260-261.
- Minami H, Ando Y, Saka H, Shimokata K. Re: prediction of carboplatin clearance from standard morphological and biological patients characteristics. *J Natl Cancer Inst*. 1997;89:968-969.
- Okamoto H, Nagamoto A, Kunitoh H, Kunikane H, Watanabe K. Prediction of carboplatin clearance calculated by patient characteristics or 24-hour creatinine clearance: a comparison of the performance of three formulae. *Cancer Chemother Pharmacol*. 1998;42:307-312.
- Donahue A, McCune JS, Faucette S, et al. Measured versus estimated glomerular filtration rate in the Carver equation: influence on carboplatin dosing. *Cancer Chemother Pharmacol*. 2001;47:373-379.
- Dooley MJ, Poole SG, Rishchin D, Webster LK. Carboplatin dosing: gender bias and inaccurate estimates of glomerular filtration rate. *Eur J Cancer*. 2002;38:44-51.
- Fukuda M, Oka M, Soda H, et al. Phase I study of irinotecan combined with carboplatin in previously untreated solid cancers. *Clin Cancer Res*. 1999;5:3963-3969.
- Ando Y, Minami H, Saka H, Ando M, Sugiura S, Sakai S, Shimokata K. Adjustment of creatinine clearance of improves accuracy of Calvert's formula for carboplatin dosing. *Br J Cancer*. 1997;76:1067-1071.
- Ozols RF. Treatment of recurrent ovarian cancer: increasing option-recurrent results. *J Clin Oncol*. 1997;15:2177-2180.
- Miller AB, Hoogstraten B, Staquet M. Reporting results of cancer treatment. *Cancer*. 1981;147:207-214.

21. Rustin GJ, Nelstrop AE, McClean P, et al. Defining response of ovarian carcinoma to initial chemotherapy according to serum CA 125. *J Clin Oncol.* 1996;14:1547-1551.
22. Tobinai K, Kohno A, Shimada Y, et al. Toxicity grading criteria of the Japan Clinical Oncology Group. *Jpn J Clin Oncol.* 1993;23:250-257.
23. Kaneda N, Nagata H, Furuta T, Yokokura T. Metabolism and pharmacokinetics of the camptothecin analogue CPT-11 in the mouse. *Cancer Res.* 1990;50:1715-1720.
24. Le Roy AF, Wehling ML, Sponseller HL, et al. Analysis of platinum in biological materials by flameless atomic absorption spectrophotometry. *Biochem Med.* 1977;18:184-191.
25. Gupta E, Lestingi TM, Mick R, Ramirez J, Vokes EE, Ratain MJ. Metabolic fate of irinotecan in humans: correlation of glucuronidation with diarrhea. *Cancer Res.* 1994;54:3723-3725.
26. Sheiner LB, Beal SL. Some suggestions for measuring predictive performance. *J Pharmacokinetic Biopharm.* 1981;9:503-512.
27. Takeda K, Negoro S, Takefuji N, et al. Dose escalation study of irinotecan combined with carboplatin for advanced non-small-cell lung cancer. *Cancer Chemother Pharmacol.* 2001;48:104-108.
28. Sato M, Ando M, Minami H, et al. Phase I/II and pharmacologic study of irinotecan and carboplatin for patients with lung cancer. *Cancer Chemother Pharmacol.* 2001;48:481-487.
29. de Jonge MJA, Verweij J, Planting AST, et al. Drug-administration sequence does not change pharmacodynamics and kinetics of irinotecan and cisplatin. *Clin Cancer Res.* 1999;5:2012-2017.
30. Sugiyama T, Yakusiji M, Kamura T, et al. Irinotecan and cisplatin as first line chemotherapy for advanced ovarian cancer. *Oncology.* 2002;63:16-22.
31. Sugiyama T, Yakushiji M, Nishida T, et al. Irinotecan combined with cisplatin in patients with refractory or recurrent ovarian cancer. *Cancer Lett.* 1998;128:211-218.
32. Kigawa J, Takahashi M, Minagawa Y, et al. Topoisomerase-1 activity and response to second-line chemotherapy consisting of camptothecin-11 and cisplatin in patients with ovarian cancer. *Int J Cancer.* 1999;84:521-524.

Relationship of the aberrant DNA hypermethylation of cancer-related genes with carcinogenesis of endometrial cancer

KOUJI BANNO*, MEGUMI YANOKURA*, NOBUYUKI SUSUMU, MAKIKO KAWAGUCHI, NOBUMARU HIRAO, AKIRA HIRASAWA, KATSUMI TSUKAZAKI and DAISUKE AOKI

Department of Obstetrics and Gynecology, Keio University School of Medicine, Tokyo, Japan

Received July 5, 2006; Accepted August 28, 2006

Abstract. Epigenetic abnormalities including the aberrant DNA hypermethylation of the promoter CpG islands play a key role in the mechanism of gene inactivation in cell carcinogenesis. To identify the genes associated with aberrant DNA hypermethylation in endometrial carcinogenesis, we studied the hypermethylation of the promoter regions of five genes: *hMLH1*, *APC*, *E-cadherin*, *RAR-β* and *p16*. The frequencies of aberrant hypermethylation were 40.4% (21/52) in *hMLH1*, 22% (11/50) in *APC*, 14% (7/50) in *E-cadherin*, and 2.3% (1/44) in *RAR-β* in endometrial cancer specimens. No aberrant DNA methylation was found in *p16*. In atypical endometrial hyperplasia, the frequencies of aberrant methylation were 14.3% (2/14) in *hMLH1* and 7.3% (1/14) in *APC*, whereas normal endometrial cells showed no aberrant hypermethylation of any of the five genes. The high frequencies of the aberrant DNA hypermethylation of *hMLH1*, *APC* and *E-cadherin* suggest that the methylation of the DNA mismatch repair and Wnt signal-related genes may be associated with endometrial carcinogenesis.

Introduction

The relationship of cellular oncogenic transformation with aberrant DNA hypermethylation in promoter regions (i.e., epigenetic changes) is an area of growing interest. Genes ranging from tumor suppressors to DNA mismatch repair and cell cycle-related genes are known to be inactivated by aberrant DNA methylation in cancer. The DNA mismatch repair genes human MutL homolog-1 (*hMLH1*) and human MutS homolog (*hMSH2*) function in the repair of base-pair

mismatches that occur in gene amplification during cell division. The characteristic seen in cancer cells when the DNA mismatch repair system breaks down is referred to as microsatellite instability (MSI). Microsatellites are repeated DNA sequences of ~1 to 5 bases, and DNA replication errors occur frequently at these sites upon the inactivation of the DNA mismatch repair genes. MSI is detected in ~40% of patients with endometrial cancer (1,2), suggesting that mutations of the DNA mismatch repair genes are associated with endometrial carcinogenesis. Therefore, in this study we examined the aberrant DNA methylation of *hMLH1*, a leading candidate in the DNA mismatch repair gene group regarding the production of MSI.

The *β-catenin* gene codes for a cell adhesion molecule that plays a key role in the Wnt signaling pathway and is generally localized in the cell membrane, where it binds to *E-cadherin*, an adhesion molecule. Free *β-catenin* forms a complex with *adenomatous polyposis coli* (*APC*) and axin is phosphorylated by GSK-3β and degraded via the proteasome pathway. The mutation of the *β-catenin* gene increases the level of undegraded *β-catenin* in the cells and causes the transition of *β-catenin* into the nucleus, which induces the activation of the Wnt signaling pathway and enhances the transcriptional activity of target genes including *cyclin D*, leading to cell cycle aberrations. The activation of the Wnt signaling pathway is also thought to be important in endometrial carcinogenesis (3), and therefore *E-cadherin* and *APC*, which are components of the Wnt signaling pathway, are also candidate genes for aberrant DNA methylation in endometrial cancer.

p16 is a tumor suppressor gene that codes for a protein that binds to CDK4 and CDK6 and inhibits the phosphorylation of the RB/E2F complex by the CDK-Cyclin D. *p16*-knockout mice develop multiple cancers in different organs, and therefore *p16* inactivation is thought to play an important role in cell carcinogenesis. The frequencies of *p16* mutation and deletion in endometrial cancer are only 5-6% and 3%, respectively (4,5), but reduced protein levels have been found in 19% of cases (5), and this may be associated with aberrant DNA methylation.

Type I endometrial cancer is also estrogen-dependent; estrogen increases the risk of endometrial cancer through a mechanism that has yet to be fully explained. Estrogen acts in a receptor-specific manner as a molecular switch to regulate transcription factor function. Estrogen receptors have highly differentiated structures, and aberrant methylation of the *estrogen receptor* (*ER*) gene in endometrial cancer has

Correspondence to: Dr Kouji Banno, Department of Obstetrics and Gynecology, Keio University School of Medicine, Shinanomachi 35, Shinjuku-ku, Tokyo 160-8582, Japan
E-mail: kbanno@sc.itc.keio.ac.jp

*Contributed equally

Key words: endometrial cancer, DNA hypermethylation, human MutL homolog-1, *E-cadherin*, *adenomatous polyposis coli*, *retinoic acid receptor-β*

Table I. Primer sequences used in MSP analysis and RT-PCR.

Gene name	PCR analysis	Sense	Antisense	Size (bp)	Ann ^a temp (°C)
<i>hMLH1</i>	Methylated	ACGTAGACGTTTTATTAGGGTCGC	CCTCATCGTAACTACCCGCG	112	60
	Unmethylated	TTTTGATGTAGATGTTTTATTAGGGTTGT	ACCACCTCATCATAACTACCCACA	124	60
<i>APC</i>	Methylated	TATTGCGGAGTGC GG GTC	TCGACGAACTCCCGACGA	100	68
	Unmethylated	GTGTTTTATTGTGGAGTGTGGGTT	CCAATCAACAAACTCCCAACAA	110	67
<i>RAR-β</i>	Methylated	GGTTAGTAGTTCGGGTAGGGTTTATC	CCGAATCCTACCCCGACG	235	59
	Unmethylated	TTAGTAGTTTGGGTAGGGTTTATT	CCAAATCCTACCCCAACA	233	59
<i>p16</i>	Methylated	TTATTAGAGGGTGGGGCGGATCGC	GACCCCGAACC GCGACCGTAA	150	67
	Unmethylated	TTATTAGAGGGTGGGGTGGATTGT	CAACCCCAAACCACAACCATAA	151	66

^aAnnealing temperature.

been reported (6). The *ER* protein shares a common fold with glucocorticoid and retinoic acid receptors (these receptors all belong to the nuclear receptor superfamily), but the frequency of the aberrant methylation of the *retinoic acid receptor-β* (*RAR-β*) gene in endometrial cancer has not been determined. However, studies of cancers in other organs (7,8) suggest a relationship between those cancers and the aberrant DNA methylation of *RAR-β*.

To identify genes associated with aberrant DNA methylation in endometrial carcinogenesis, we studied the aberrant DNA methylation of the promoter regions of five genes (*hMLH1*, *APC*, *E-cadherin*, *RAR-β* and *p16*) that show high frequencies of aberrant DNA methylation in different cancers and may be important in endometrial carcinogenesis.

Materials and methods

Clinical specimens. The subjects were 93 patients who gave informed consent to the collection of endometrial specimens (27 normal endometria, 14 atypical endometrial hyperplasia, and 52 endometrial cancers). The cells obtained from the tissue specimens were examined by liquid-based cytology using the ThinPrep system (Cytoc Corporation, Boxborough, MA, USA) with preservation fluid (PreservCyt Solution, Cytoc Corporation) (9). A pathological diagnosis of the endometrial tissue was consistent with the cytology results for all the 93 subjects. Of the 27 patients with a normal endometrium, 16 were in the secretory phase and 11 were in the proliferative phase. Of the 52 patients with endometrial cancer, 44 had ovarian endometrioid adenocarcinoma (G1, 24; G2, 10; G3, 10) and 8 had adenosquamous carcinoma. The grade of histological differentiation (G1 to G3) and the cancer stage at surgery were determined based on the Guidelines for Endometrial Cancer published by the Japan Society of Obstetrics and Gynecology.

DNA extraction and methylation-specific PCR (MSP) analysis. DNA was extracted from 93 endometrial specimens using liquid-based cytology with a Get Pure DNA kit (Dojindo Molecular Technologies Inc., Kumamoto, Japan). Distilled

water was added to 1 μg of the extracted DNA up to a volume of 50 μl, 5.5 μl 3 N NaOH solution was added, and, after mixing, the solution was incubated at 37°C for 15 min. Following this, 520 μl 3 M sodium bisulfite (Sigma, St. Louis, MO, USA), which was prepared at pH 5.5 with 30 μl 10 mM hydroquinone (Sigma) and 10 N NaOH, was added to the solution. After mixing in an upturned position to prevent vaporization, the solution was overlaid with mineral oil and incubated at 50°C overnight. Next, 1 ml clean-up resin (Promega Corporation, Madison, WI, USA) was added to the lower layer, and the resulting solution was mixed in an upturned position and then injected into a column. After rinsing with 2 ml 80% isopropanol, the column was centrifuged at 15,000 rpm for 3 min to remove the isopropanol completely, after which 50 μl distilled water (70°C) was added directly to the column, and the column was centrifuged at 15,000 rpm for 2 min to extract the DNA adsorbed in the column. Then, 5.5 μl 2 N NaOH was added to the resulting DNA solution, and, after mixing, the solution was incubated at 37°C for 20 min, after which 66 μl 5 N ammonium acetate solution and 243 μl 95% ethanol were added, and the solution was incubated at 80°C for 1 h and centrifuged at 15,000 rpm for 30 min to precipitate the DNA. Approximately 50 μl of the supernatant was left in the tube, and the rest of the supernatant was collected, mixed with 1 ml 70% ethanol, and then centrifuged at 15,000 rpm for 30 min to rinse the DNA. The precipitated DNA was air-dried and dissolved in 20 μl distilled water; 2 μl of this solution was used as the MSP template solution. AmpliTaq Gold & 10X PCR buffer/MgCl₂ with dNTP (Applied Biosystems, Foster City, CA, USA) was used in the PCR analysis, and the DNA was analyzed using a GeneAmp PCR 9700 system (Applied Biosystems). A CpG WIZ *E-cadherin* amplification kit (Chemicon, Temecula, CA, USA) was used as the MSP for the *E-cadherin* gene. The PCR conditions and primer sequences for the other genes are shown in Table I.

Immunohistochemical analysis of endometrial cancer tissues. Twenty surgical endometrial specimens from 52 patients were examined using liquid-based cytology. Formalin-fixed,

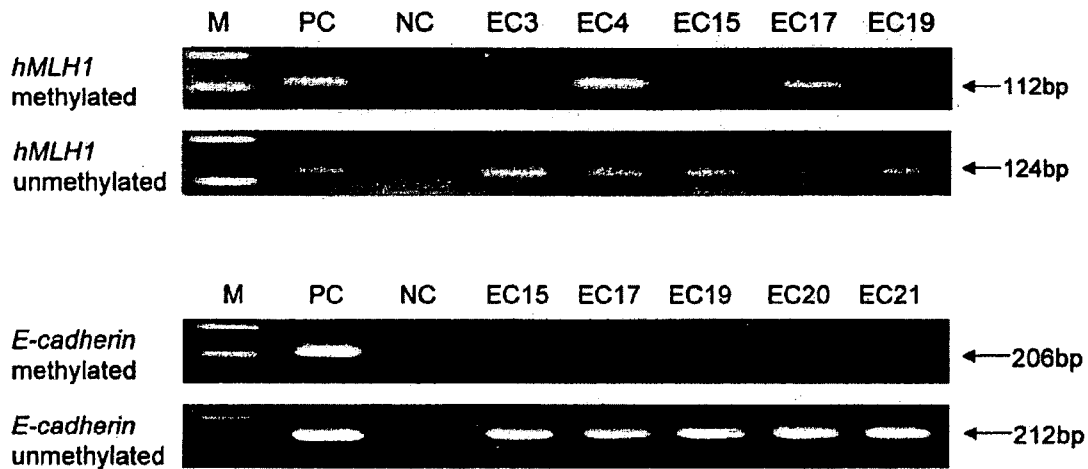


Figure 1. MSP analysis of the *hMLH1* and *E-cadherin* genes in endometrial cancer specimens. MSP analysis was conducted using DNA extracted from endometrial cancer specimens. The results for *hMLH1* and *E-cadherin* are shown in the upper and lower panels, respectively. For *hMLH1* the aberrant methylation band is shown in lanes EC4 and EC17, and for *E-cadherin* this band is shown in lanes EC20 and EC21. M, marker; PC, positive control; NC, negative control; EC, endometrial cancer.

paraffin-embedded specimens were prepared and the slices were stained in a silane-coated slide using a Vectastain ABC kit (Vector Laboratories, Burlingame, CA, USA). After deparaffinizing, the slides were heated in 10 mM citric acid buffer solution (pH 7.0) at 120°C for 10 min in an autoclave for antigen retrieval. After allowing the slides to cool to room temperature, intrinsic peroxidase activity was eliminated by treating the slides with 3% H₂O₂ in phosphate-buffered saline (PBS) for 5 min. The slides were rinsed twice with PBS and blocked with normal goat serum, and then rinsed twice again with PBS and diluted with 1% bovine serum albumin (BSA) in PBS and incubated with the primary antibody at 4°C overnight. The primary antibodies were the 50-fold diluted anti-*hMLH1* antibody (BD Bioscience Pharmingen, San Diego, CA, USA) and the 500-fold diluted anti-*E-cadherin* antibody (Takara, Tokyo, Japan). After rinsing three times with PBS, the slides were incubated with the secondary antibody (biotin-labeled anti-mouse IgG) at room temperature for 30 min. After rinsing three more times with PBS, the slides were incubated with ABC (avidin-biotin peroxidase) complex at room temperature for 30 min. After further rinsing three times with PBS, the slides were treated with 0.2 mg/ml diaminobenzidine (DAB) for about 5 min for coloring. After rinsing twice with PBS, the slides were treated with hematoxylin solution for nuclear staining, and then dehydrated and observed microscopically. For judging the immunohistochemical staining intensity of the *hMLH1* protein, the nuclei of endometrial stromal cells were used as an internal control; if the nuclei of the tumor cells containing the protein showed a stronger staining intensity than the control nuclei, the specimen was considered positive, whereas a specimen was considered negative if the tumor cell nuclei showed a lower staining intensity than the control nuclei (10). Regarding the *E-cadherin* staining, the protein is localized in the cell membrane in normal epithelial cells, and the immunohistochemical analysis was conducted in accordance with the criteria of Wu *et al.*: Specimens with $\geq 25\%$ of the tumor cells that stained for *E-cadherin* in the

cell membrane were considered positive, and specimens with $< 25\%$ of the tumor cells giving this staining result were considered negative (11).

Statistical analysis. The correlation of the aberrant DNA methylation of the *hMLH1*, *APC* and *E-cadherin* genes with the clinicopathological factors, grade of histological differentiation and cancer stage at surgery was analyzed using Mann-Whitney tests. The correlation of the aberrant DNA methylation of each of these genes with the patients' age was also examined, after confirming that the groups of patients with and without aberrant methylation showed a normal age distribution based on a normal distribution test. An F test was used to confirm that the population variances of the two independent groups were equal to each other, and then the differences in the population means were examined using the Student's t-test. The correlation of the aberrant DNA methylation level of *hMLH1* with those of *APC*, *E-cadherin* and *RAR- β* , respectively, was calculated using Fisher's exact test, and the correlations of the aberrant DNA methylation of *hMLH1* and *E-cadherin* with the immunohistochemical staining data were also examined using Fisher's exact test.

Results

Aberrant DNA methylation of cancer-related genes in endometrial specimens. Fig. 1 shows partial results of the MSP analysis of the endometrial cancer cells obtained using liquid-based cytology. A band due to the aberrant methylation of the *hMLH1* gene was present in samples EC4 and EC17 (size, 112 bp), and bands due to the aberrant methylation of *E-cadherin* were found in samples EC20 and EC21 (206 bp). MSP analysis of the endometrial cancer specimens indicated that the frequencies of the aberrant methylation of the promoter regions were 40.4% (21/52) for *hMLH1*, 22% (11/50) for *APC*, 14% (7/50) for *E-cadherin*, and 2.3% (1/44) for *RAR- β* . No aberrant methylation was found in the promoter region of the

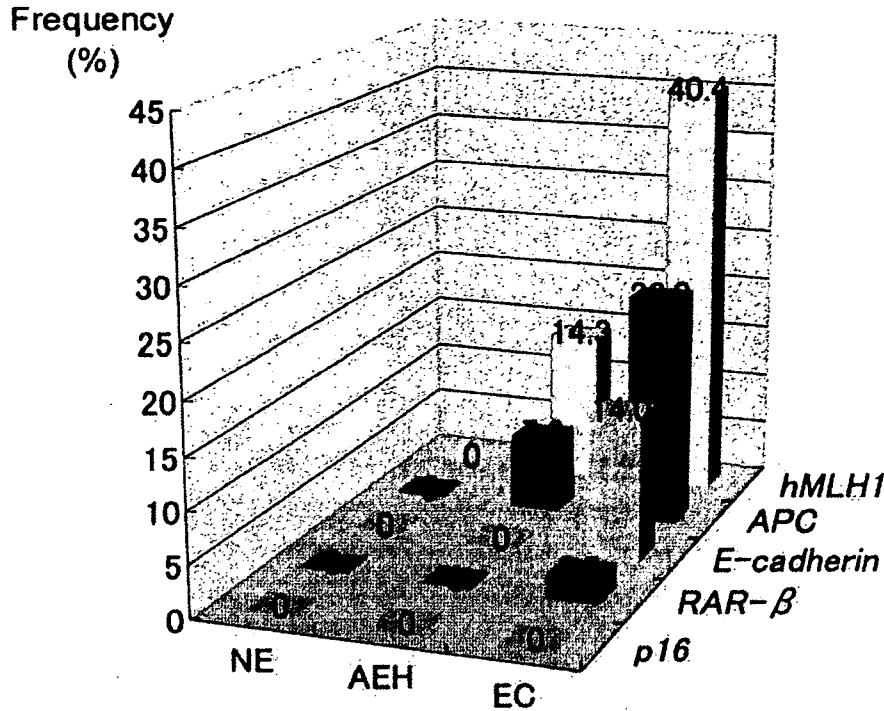


Figure 2. Frequencies of aberrant methylation of cancer-related genes in specimens from normal endometria, atypical endometrial hyperplasia and endometrial cancer. In the endometrial cancer specimens, *hMLH1* exhibited the highest frequency of aberrant methylation, followed by *APC* and *E-cadherin*. Aberrant methylation of *hMLH1* was also found in atypical endometrial hyperplasia, whereas normal endometrial cells showed no aberrant methylation of the five genes. NE, normal endometrium; AEH, atypical endometrial hyperplasia; EC, endometrial cancer.

Case	Age	Tissue type	Cancer stage	Differentiation grade	<i>hMLH1</i>	<i>E-cad</i>	<i>APC</i>	<i>RAR-β</i>	<i>p16</i>
EC1	52	endometrioid adenocarcinoma	I b	G3					
EC2	80	endometrioid adenocarcinoma	I a	G1					
EC3	51	endometrioid adenocarcinoma	III c	G1					
EC4	54	adenosquamous carcinoma	III c	G3					
EC5	51	endometrioid adenocarcinoma	I a	G1					
EC6	81	endometrioid adenocarcinoma	I b	G1					
EC7	70	endometrioid adenocarcinoma	III c	G2					
EC8	81	endometrioid adenocarcinoma	II b	G1					
EC9	62	adenosquamous carcinoma	III a	G2					
EC10	40	endometrioid adenocarcinoma	II a	G1					
EC11	59	endometrioid adenocarcinoma	II a	G3					
EC12	57	endometrioid adenocarcinoma	I b	G3					
EC13	80	endometrioid adenocarcinoma	III c	G3					
EC14	54	adenosquamous carcinoma	I b	G1					
EC15	53	endometrioid adenocarcinoma	I b	G3					
EC16	42	endometrioid adenocarcinoma	II b	G1					
EC17	71	endometrioid adenocarcinoma	III c	G3					
EC18	80	endometrioid adenocarcinoma	I b	G1					
EC19	57	endometrioid adenocarcinoma	III a	G2					
EC20	71	endometrioid adenocarcinoma	II a	G1					
EC21	37	endometrioid adenocarcinoma	II a	G2					
EC22	47	endometrioid adenocarcinoma	III b	G1					
EC23	87	endometrioid adenocarcinoma	I c	G2					
EC24	53	endometrioid adenocarcinoma	I a	G1					
EC25	69	endometrioid adenocarcinoma	III c	G2					
EC26	56	endometrioid adenocarcinoma	III c	G2					
EC27	54	endometrioid adenocarcinoma	I a	G1					
EC28	83	endometrioid adenocarcinoma	I a	G1					
EC29	41	endometrioid adenocarcinoma	I b	G1					
EC30	62	adenosquamous carcinoma	I b	G1					
EC31	58	endometrioid adenocarcinoma	I b	G2					
EC32	56	endometrioid adenocarcinoma	III c	G3					
EC33	71	endometrioid adenocarcinoma	I b	G2					
EC34	53	adenosquamous carcinoma	I b	G3					
EC35	50	endometrioid adenocarcinoma	III a	G3					
EC36	42	adenosquamous carcinoma	III c	G3					
EC37	53	endometrioid adenocarcinoma	I c	G3					
EC38	34	adenosquamous carcinoma	III c	G1					
EC39	61	endometrioid adenocarcinoma	I c	G1					
EC40	61	endometrioid adenocarcinoma	I c	G1					
EC41	61	endometrioid adenocarcinoma	I b	G1					
EC42	69	endometrioid adenocarcinoma	I b	G1					
EC43	65	adenosquamous carcinoma	IV b	G2					
EC44	54	endometrioid adenocarcinoma	II a	G1					
EC45	57	endometrioid adenocarcinoma	II a	G1					
EC46	56	endometrioid adenocarcinoma	I b	G2					
EC47	76	endometrioid adenocarcinoma	I b	G3					
EC48	65	endometrioid adenocarcinoma	I b	G2					
EC49	37	endometrioid adenocarcinoma	I a	G1					
EC50	36	endometrioid adenocarcinoma	I a	G1					
EC51	26	endometrioid adenocarcinoma	I a	G1					
EC52	18	endometrioid adenocarcinoma	I a	G1					


Figure 3. Aberrant methylation of the promoter regions of cancer-related genes in endometrial cancer. G1, well-differentiated; G2, moderately differentiated; G3, poorly differentiated; EC, endometrial cancer; *E-cad*, *E-cadherin*.

p16 gene. In the atypical endometrial hyperplasia samples, the frequencies of the aberrant methylation of the promoter regions were 14.3% (2/14) for *hMLH1* and 7.3% (1/14) for *APC*.


Normal endometrial cells in the proliferative and secretory phases showed no aberrant methylation of the promoter regions of the five examined genes (Figs. 2-4).

Case	Age	Tissue type	<i>hMLH1</i>	<i>E-cad</i>	<i>APC</i>	<i>RAR-β</i>	<i>p16</i>
NE1	37	sec					
NE2	43	sec					
NE3	51	sec					
NE4	35	sec					
NE5	39	sec					
NE6	41	sec					
NE7	47	sec					
NE8	40	sec					
NE9	36	sec					
NE10	49	sec					
NE11	51	sec					
NE12	52	sec					
NE13	44	sec					
NE14	47	sec					
NE15	23	sec					
NE16	34	sec					
NE17	37	pro					
NE18	37	pro					
NE19	51	pro					
NE20	49	pro					
NE21	43	pro					
NE22	36	pro					
NE23	43	pro					
NE24	42	pro					
NE25	27	pro					
NE26	44	pro					
NE27	32	pro					

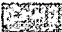
Case	Age	<i>hMLH1</i>	<i>E-cad</i>	<i>APC</i>	<i>RAR-β</i>	<i>p16</i>
AEH1	34					
AEH2	30					
AEH3	32					
AEH4	35					
AEH5	35					
AEH6	46					
AEH7	41					
AEH8	33					
AEH9	41					
AEH10	50					
AEH11	45					
AEH12	47					
AEH13	45					
AEH14	33					



Methylated



Unmethylated



Not done

Figure 4. Aberrant methylation of the promoter regions of cancer-related genes in atypical endometrial hyperplasia. AEH, atypical endometrial hyperplasia; *E-cad*, *E-cadherin*.

Immunohistochemical analysis of *hMLH1* and *E-cadherin* protein expression. The relationship of the aberrant DNA methylation of the promoter regions of the *hMLH1* and *E-cadherin* genes with protein expression was determined immunohistochemically. Of the 20 surgical specimens of endometrial cancer showing aberrant methylation, most showed negative protein staining (*hMLH1*, $p < 0.01$; *E-cadherin*, $p < 0.05$) (Fig. 5) (Table II).

Correlation of aberrant DNA methylation of cancer-related genes with clinicopathological factors. The correlations of the aberrant DNA methylation of the promoter regions of *hMLH1*, *APC* and *E-cadherin* with the clinicopathological factors were examined in endometrial cancer patients. For the *hMLH1*, *APC* and *E-cadherin* genes, no correlation was found between aberrant methylation and the grade of histological differentiation or with cancer stage at surgery. Aberrant DNA methylation is generally thought to increase with age, but no significant difference was found in the mean age between patients with and without aberrant methylation of *hMLH1*, *APC* and *E-cadherin*, respectively. Therefore, these data do not indicate that aberrant methylation occurs more frequently in elderly patients with endometrial cancer (Table IV).

The relationship of the aberrant methylation of the promoter region of *hMLH1*, which showed the highest frequency in the endometrial cancer samples, was also

examined with that of other genes, but no correlation was found with the methylation of *APC*, *E-cadherin* or *RAR-β*.

Discussion

Of the five endometrial cancer-related genes examined, the aberrant methylation of *hMLH1*, a DNA mismatch repair gene, was found most frequently (40.4%). The frequencies of the aberrant methylation of *hMLH1* have been reported as 14% to 26% in gastric cancer (12,13) and 7% to 32% in lung cancer (14,15); therefore, the frequency of the aberrant methylation of this gene in endometrial cancer is higher than in other cancers. After *hMLH1*, the second most likely genes to show aberrant methylation were *APC* and *E-cadherin*, which are Wnt-related genes. Collectively, these data suggest that abnormal DNA mismatch repair and aberrant Wnt signaling are associated with endometrial carcinogenesis. However, patients with an aberrant methylation of *hMLH1* rarely corresponded to those with an aberrant methylation of *E-cadherin*, and therefore carcinogenesis due to the aberrant methylation of these respective genes may occur through independent mechanisms.

The aberrant methylation of *hMLH1* may cause a reduced protein expression that leads to abnormal DNA mismatch repair and MSI. However, although MSI has been found in ~40% of patients with endometrial cancer, the *hMLH1*

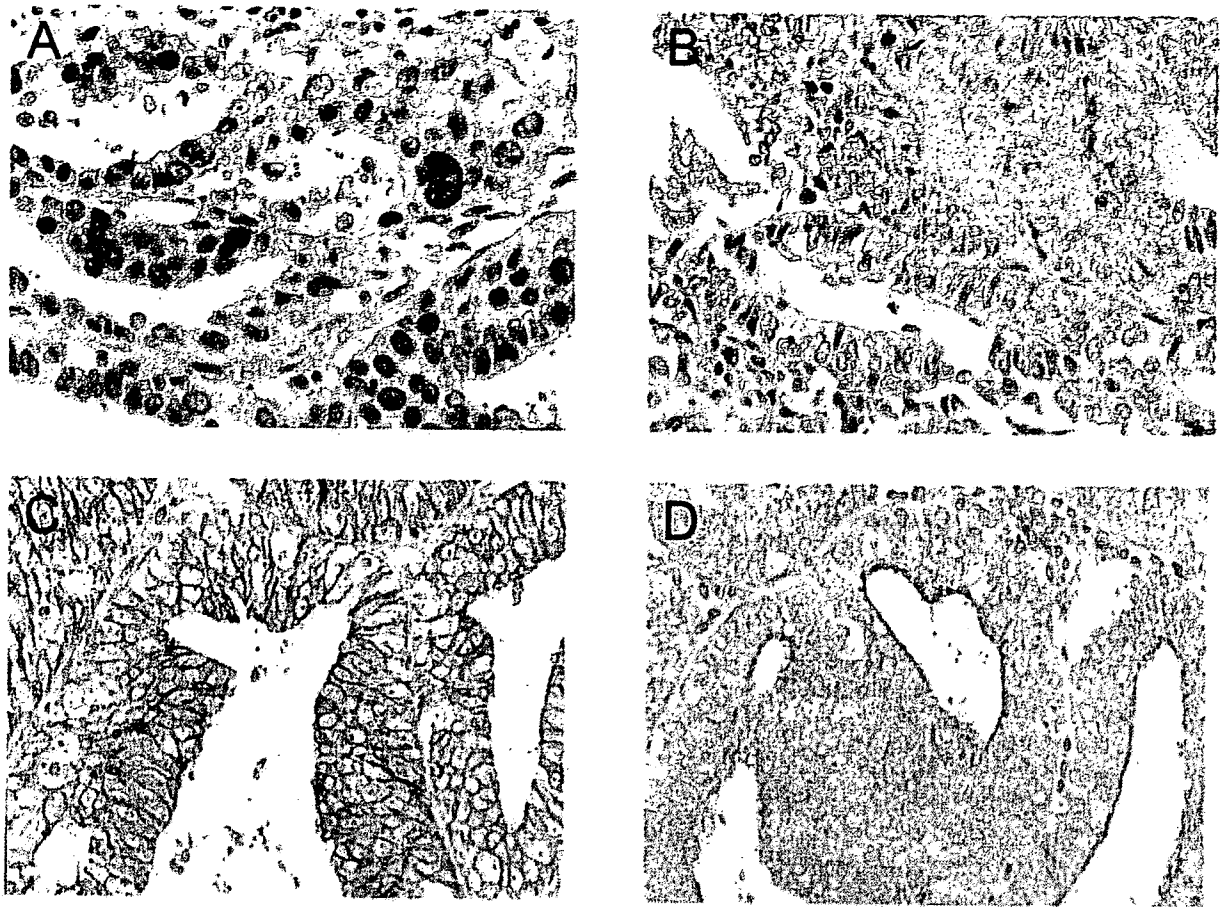


Figure 5. (A and B) Immunohistochemical analysis of the endometrial cancer specimens using the anti-*hMLH1* antibody. (A) In patients with an unmethylated *hMLH1* gene (EC23), the nuclei of the cancer cells were strongly stained. (B) In patients with aberrant methylation of *hMLH1* (EC31), the cell nuclei were less strongly stained. (C and D) Immunohistochemical analysis of the endometrial cancer specimens using the anti-*E-cadherin* antibody. (C) In patients with unmethylated *E-cadherin* (EC29), the cell membranes of the cancer cells were strongly stained. (D) In patients with aberrant methylation of *E-cadherin* (EC8), the cell membranes were less strongly stained. EC, endometrial cancer.

Table II. Relationship of the aberrant DNA methylation of the *hMLH1* and *E-cadherin* genes with reduced protein expression.

	Expressed	Not expressed	
<i>hMLH1</i>			
methylated	3	9	p<0.01
unmethylated	8	0	
<i>E-cadherin</i>			
methylated	2	2	p<0.05
unmethylated	15	1	

mutation frequency in MSI-positive endometrial cancer patients is extremely low (16,17), suggesting that MSI may occur due to the aberrant methylation of the promoter regions, and not due to the *hMLH1* mutation. Furthermore, the aberrant methylation of *hMLH1* has been found in atypical endometrial hyperplasia, but is not observed in the normal endometrium;

Table III. Correlation of the aberrant DNA methylation of cancer-related genes with the grade of histological differentiation and clinical stage at surgery.

	G1	G2	G3	Stage			
				I	II	III	IV
<i>hMLH1</i>							
M	12	6	3	11	4	5	1
U	15	6	10	19	4	8	0
<i>E-cadherin</i>							
M	4	1	2	3	3	1	0
U	22	11	10	24	5	13	1
<i>APC</i>							
M	5	2	4	7	2	2	0
U	21	10	8	20	6	12	1

G1, well-differentiated; G2, moderately differentiated; G3, poorly differentiated; M, methylated; U, unmethylated.

Table IV. Correlation of the aberrant DNA methylation of cancer-related genes with the mean onset age of endometrial cancer.

	<i>hMLH1</i>		<i>E-cadherin</i>		<i>APC</i>		<i>RAR-β</i>
Methylated	53.3±11.46] NS	59.6±13.78] NS	59.7±9.37] NS	55
Unmethylated	55.7±12.78		54.9± 10.84		54.3±11.57		56.26±9.76

NS, not significant.

therefore, aberrant methylation occurs in the early stage of carcinogenesis. Since such aberrant methylation can be detected in a small amount of cytological material by using minimally invasive procedures, the determination of the methylation levels of genes such as *hMLH1* is a potential supplementary diagnostic method for endometrial cancer.

An accumulation of β -catenin in the nucleus, which indicates aberrant Wnt-signaling, has been observed in 23.8% of patients with endometrial cancer (18), and is thought to be one of the causes of endometrial cancer. In contrast, the β -catenin mutation frequency is only 11%, significantly lower than the frequency of the accumulation of β -catenin in the nucleus (18). Furthermore, the accumulation of β -catenin in the nucleus has been observed in patients without β -catenin mutations; therefore, the transition and accumulation of β -catenin in the nucleus are dependent on a mechanism other than gene mutation. The aberrant methylation of the promoter region of *E-cadherin*, which codes for a scaffolding protein that binds to β -catenin and is present in the cell membrane as a cell adhesion molecule, was found in 14% of the patients with endometrial cancer in our patient population. Reduced levels of the *E-cadherin* protein were frequently observed in the patients with aberrant methylation of *E-cadherin*, suggesting that the inactivation of *E-cadherin* by aberrant methylation could be associated with changes in the localization of β -catenin in endometrial cancer. The aberrant methylation of *E-cadherin* has also been found in G3 adenocarcinoma (19), but no correlation with the localization of β -catenin has been investigated. The aberrant methylation of *E-cadherin* was not detected in the patients with atypical endometrial hyperplasia, which is considered pathologically to be Stage 0 endometrial cancer, but was found in the patients with Stage Ia or higher endometrial cancer. This suggests that the aberrant methylation of *E-cadherin* is not involved in early-stage carcinogenesis, in contrast to *hMLH1*.

Similar to the aberrant methylation of the *hMLH1* gene, the aberrant methylation of *APC*, a component of the Wnt signaling pathway, was observed in 7.3% of the patients with atypical endometrial hyperplasia and 22% of the patients with endometrial cancer; however, no reduction in the levels of the *APC* protein was observed. Therefore, our results indicate that there is no relationship between the inactivation of *APC* by aberrant methylation and the onset of endometrial cancer.

The frequencies of the aberrant methylation of *RAR-β* and *p16* were 2.3% and 0% in the endometrial cancer patients, respectively, which are significantly lower than those in

cancers of other organs. These results suggest that the type and frequency of genes undergoing aberrant methylation in endometrial cancer are specific and differ from those in other cancers. The aberrant methylation of the promoter region of *p16* has been reported in 20% of non-Japanese patients with endometrial cancer (20); the difference between this result and our study suggests that the frequencies of aberrant DNA methylation in endometrial cancer may also vary between races. Furthermore, aging is generally thought to be an important factor for aberrant DNA methylation, but we found no tendency for increased aberrant methylation in elderly patients with endometrial cancer. The mechanism of the induction of aberrant DNA methylation may also differ widely between organs and tissues (21), and this may account for the differences in results between the studies.

Acknowledgements

This study was partially supported by the Ministry of Education, Culture, Sports, Science and Technology through a Grant-in-Aid for Scientific Research (17791135), and by the Public Trust Haraguchi Memorial Cancer Research Fund. We are grateful to the Cytoc Corporation for the provision of ThinPrep.

References

1. Esteller M, Catusas L, Matias-Guiu X, Mutter GL, Prat J, Baylin SB and Herman JG: *hMLH1* promoter hypermethylation is an early event in human endometrial tumorigenesis. *Am J Pathol* 155: 1767-1772, 1999.
2. Kanaya T, Kyo S, Maida Y, Yatabe N, Tanaka M, Nakamura M and Inoue M: Frequent hypermethylation of *MLH1* promoter in normal endometrium of patients with endometrial cancers. *Oncogene* 22: 2352-2360, 2003.
3. Fukuchi T, Sakamoto M, Tsuda H, Maruyama K, Nozawa S and Hirohashi S: Beta-catenin mutation in carcinoma of the uterine endometrium. *Cancer Res* 58: 3526-3528, 1998.
4. Peiffer SL, Bartsch D, Whelan AJ, Mutch DG, Herzog TJ and Goodfellow PJ: Low frequency of *CDKN2* mutation in endometrial carcinomas. *Mol Carcinog* 13: 210-212, 1995.
5. Nakashima R, Fujita M, Enomoto T, Haba T, Yoshino K, Wada H, Kurachi H, Sasaki M, Wakasa K, Inoue M, Buzard G and Murata Y: Alteration of *p16* and *p15* genes in human uterine tumours. *Br J Cancer* 80: 458-467, 1999.
6. Sasaki M, Dharia A, Oh BR, Tanaka Y, Fujimoto S and Dahiya R: Progesterone receptor B gene inactivation and CpG hypermethylation in human uterine endometrial cancer. *Cancer Res* 61: 97-102, 2001.
7. Widschwendter M, Berger J, Hermann M, Muller HM, Amberger A, Zeschnick M, Widschwendter A, Abendstein B, Zeimet AG, Daxenbichler G and Marth C: Methylation and silencing of the retinoic acid receptor-beta2 gene in breast cancer. *J Natl Cancer Inst* 92: 826-832, 2000.

8. Ueki T, Toyota M, Skinner H, Walter KM, Yeo CJ, Issa JP, Hruban RH and Goggins M: Identification and characterization of differentially methylated CpG islands in pancreatic carcinoma. *Cancer Res* 61: 8540-8546, 2001.
9. Susumu N, Aoki D, Noda T, Nagashima Y, Hirao T, Tamada Y, Banno K, Suzuki A, Suzuki N, Tsuda H, Inazawa J and Nozawa S: Diagnostic clinical application of two-color fluorescence *in situ* hybridization that detects chromosome 1 and 17 alterations to direct touch smear and liquid-based thin-layer cytologic preparations of endometrial cancers. *Int J Gynecol Cancer* 15: 70-80, 2005.
10. Banno K, Susumu N, Hirao T, Yanokura M, Hirasawa A, Aoki D, Udagawa Y, Sugano K and Nozawa S: Two Japanese kindreds occurring endometrial cancer meeting new clinical criteria for hereditary non-polyposis colorectal cancer (HNPCC), Amsterdam Criteria II. *J Obstet Gynaecol Res* 30: 287-292, 2004.
11. Wu ZY, Zhan WH, Li JH, He YL, Wang JP, Lan P, Peng JS and Cai SR: Expression of E-cadherin in gastric carcinoma and its correlation with lymph node micrometastasis. *World J Gastroenterol* 11: 3139-3143, 2005.
12. Oue N, Oshimo Y, Nakayama H, Ito R, Yoshida K, Matsusaki K and Yasui W: DNA methylation of multiple genes in gastric carcinoma: association with histological type and CpG island methylator phenotype. *Cancer Sci* 94: 901-905, 2003.
13. Hong SH, Kim HG, Chung WB, Kim EY, Lee JY, Yoon SM, Kwon JG, Sohn YK, Kwak EK and Kim JW: DNA hypermethylation of tumor-related genes in gastric carcinoma. *J Korean Med Sci* 20: 236-241, 2005.
14. Chen G, Liu T and He J: Status of methylation of promoter of mismatch repair gene hMLH1 in lung cancer. *Chung Hua Chung Liu Tsa Chih* 22: 493-495, 2000.
15. Yanagawa N, Tamura G, Oizumi H, Takahashi N, Shimazaki Y and Motoyama T: Promoter hypermethylation of tumor suppressor and tumor-related genes in non-small cell lung cancers. *Cancer Sci* 94: 589-592, 2003.
16. Baldinu P, Cossu A, Manca A, Satta MP, Pisano M, Casula M, Dessole S, Pintus A, Tanda F and Palmieri G: Microsatellite instability and mutation analysis of candidate genes in unselected Sardinian patients with endometrial carcinoma. *Cancer* 94: 3157-3168, 2002.
17. Kowalski LD, Mutch DG, Herzog TJ, Rader JS and Goodfellow PJ: Mutational analysis of MLH1 and MSH2 in 25 prospectively-acquired RER+ endometrial cancers. *Genes Chromosomes Cancer* 18: 219-227, 1997.
18. Moreno-Bueno G, Hardisson D, Sanchez C, Sarrío D, Cassia R, Garcia-Rostan G, Prat J, Guo M, Herman JG, Matias-Guiu X, Esteller M and Palacios J: Abnormalities of the APC/beta-catenin pathway in endometrial cancer. *Oncogene* 21: 7981-7990, 2002.
19. Saito T, Nishimura M, Yamasaki H and Kudo R: Hypermethylation in promoter region of E-cadherin gene is associated with tumor dedifferentiation and myometrial invasion in endometrial carcinoma. *Cancer* 97: 1002-1009, 2003.
20. Wong YF, Chung TK, Cheung TH, Nobori T, Yu AL, Batova A, Lai KW and Chang AM: Methylation of p16INK4A in primary gynecologic malignancy. *Cancer Lett* 136: 231-235, 1999.
21. Yanokura M, Banno K, Susumu N, Kwaguchi M, Kuwabara Y, Tsukazaki K and Aoki D: Hypermethylation in the p16 promoter region in the carcinogenesis of endometrial cancer in Japanese patients. *Anticancer Res* 26: 851-856, 2006.

Relationship of aberrant DNA hypermethylation of *CHFR* with sensitivity to taxanes in endometrial cancer

MEGUMI YANOKURA*, KOUJI BANNO*, MAKIKO KAWAGUCHI, NOBUMARU HIRAO, AKIRA HIRASAWA, NOBUYUKI SUSUMU, KATSUMI TSUKAZAKI and DAISUKE AOKI

Department of Obstetrics and Gynecology, Keio University School of Medicine, Tokyo, Japan

Received August 31, 2006; Accepted October 9, 2006

Abstract. The relationship of aberrant DNA hypermethylation of cell cycle checkpoint genes with the sensitivity of cancer cells to anticancer drugs is a question of current interest. In this study, we investigated the relationship between aberrant hypermethylation of the *CHFR* (checkpoint with forkhead-associated and ring finger) mitotic checkpoint gene and sensitivity to taxanes in endometrial cancer. Methylation-specific PCR (MSP) indicated aberrant hypermethylation of *CHFR* in 12.0% (6/50) of endometrial cancer specimens, and suggested that aberrant hypermethylation is significantly more frequent in poorly differentiated adenocarcinoma (G3) ($p < 0.05$). Of six culture cell lines, SNG-II and HEC108 cells showed aberrant hypermethylation and reduced expression of *CHFR*. These cells had high sensitivity to taxanes but became resistant after demethylation. Cancer specimens with aberrant hypermethylation of *CHFR* also exhibited high sensitivity to taxanes. To our knowledge, this study is the first to examine aberrant hypermethylation of *CHFR* in endometrial cancer, and our results suggest that the methylation status of *CHFR* may be a new molecular index that will allow design of personalized treatment in endometrial cancer. This may be particularly important in poorly differentiated adenocarcinoma (G3), which is known to have a poor prognosis.

Introduction

Recent studies have shown that aberrant DNA hypermethylation of cell cycle checkpoint genes in cancer cells has a major effect on specific anticancer drugs (1,2). The *CHFR* (checkpoint with forkhead-associated and ring finger) mitotic

checkpoint gene is located in 12q24.33 and has the function of delaying chromatin condensation and progression to the mitotic phase (3). The *CHFR* protein has a forkhead-associated domain in the N-terminal region and a finger domain in the central region; these two domains act as a sensor for mitotic stress and therefore function as a cell cycle M phase checkpoint. Upon detection of mitotic stress in a cell, *CHFR* action causes arrest of the cell cycle in G2 phase to allow repair of damaged DNA (G2 arrest).

Taxanes are anticancer agents that act in M phase as microtubule depolymerization inhibitors. Upon administration of a taxane to cancer cells, those cells with normal *CHFR* develop G2 arrest and repair damaged DNA, thereby exhibiting resistance to taxanes. In contrast, cells with inactivated *CHFR* due to aberrant hypermethylation proceed with the cell cycle due to failed detection of damaged DNA and subsequently cannot go on to normal cell division, leading to mitotic catastrophe and cell death; i.e., these cells show high sensitivity to taxanes. Given this background, the methylation status of *CHFR* is likely to be a highly sensitive molecular index for taxane sensitivity of cancer cells.

A relationship between aberrant hypermethylation of *CHFR* and sensitivity to taxanes has been reported in colon and gastric cancer cells in culture (2,4), but not in endometrial cancer. Therefore, we investigated this relationship in endometrial cancer, with the goal of establishing a molecular index that might lead to personalized treatment strategies for endometrial cancer.

Materials and methods

Subjects and specimens for biopsy. The subjects were 69 patients who gave informed consent for collection of endometrial specimens (9 of normal endometrium, 10 of atypical endometrial hyperplasia and 50 of endometrial cancer). Cells obtained from the tissue specimens were examined by liquid-based cytology using the ThinPrep System (Cytoc Corp., Boxborough, MA) with preservation fluid (PreservCyt Solution, Cytoc Corp.) (5). A pathological diagnosis of the endometrial tissue was consistent with cytology results for all 69 subjects. Of the 9 patients with a normal endometrium, 5 were in the secretory phase and 4 were in the proliferative phase, and of the 50 patients with endometrial cancer, 42 had ovarian endometrioid adenocarcinoma (G1, 20; G2, 12; G3, 10) and 8 had adenosquamous carcinoma. The grade of histo-

Correspondence to: Dr Kouji Banno, Department of Obstetrics and Gynecology, Keio University School of Medicine, Shinanomachi 35, Shinjuku-ku, Tokyo 160-8582, Japan
E-mail: kbanno@sc.itc.keio.ac.jp

*Contributed equally

Key words: *CHFR*, endometrial cancer, DNA hypermethylation, taxane, chemosensitivity

Table I. Primer sequences used in MSP and RT-PCR analyses.

Gene name	PCR analysis	Sense	Antisense	Size (bp)	Annealing temperature (°C)
<i>CHFR</i>	Methylated	GTCGGGTCGGGGTTC	CCCAAACTACGACGACG	150	60
	Unmethylated	ATATAATATGGTGTGATT	TCAACTAATCCACAAAACA	206	53
<i>CHFR</i>	RT-PCR	TGGAACAGTGATTAACAAGC	AGGTATCTTTGGTCCCATGG	206	55
<i>β-actin</i>	RT-PCR	TTATTTGAGCTTTGGTTCTG	CTCCTTAATGTCACGCACGATTC	303	50

logical differentiation (G1-G3) and the cancer stage at surgery were determined based on the Guidelines for Endometrial Cancer published by the Japan Society of Obstetrics and Gynecology.

Culture cell lines. Six cell strains were used: HEC108 (a human endometrial cancer-derived culture cell line supplied by Dr Hiroyuki Kuramoto), HOOUA and HHUA (supplied by Dr Isamu Ishiwata) and SNG-II, HEC1B and KLE. KLE cells were cultured in a DMEM/F12 (1:1) medium (Gibco BRL, Rockville, MD, USA) supplemented with 10% fetal bovine serum (FBS) (Sanko Junyaku Co., Ltd., Tokyo, Japan), and the other cells were cultured in 10% FBS-supplemented F12 medium (Sigma, St. Louis, MO, USA). The cells were incubated in a 10-cm dish under 5% CO₂ at 37°C.

DNA extraction and methylation-specific PCR (MSP) analysis of *CHFR*. DNA was extracted from 69 endometrial specimens and 6 endometrial cancer-derived cell lines using liquid-based cytology with a GetPure DNA Kit (Dojindo Molecular Technologies, Inc., Kumamoto, Japan). Distilled water was added to 1 µg of the extracted DNA up to a volume of 50 µl, 5.5 µl of 3 N NaOH solution was added, and after mixing the solution was incubated at 37°C for 15 min. Following this, 520 µl of 3 M sodium bisulfate (Sigma), which was prepared at pH 5.5 with 30 µl of 10 mM hydroquinone (Sigma) and 10 N NaOH, was added to the solution. After mixing in an upturned position to prevent vaporization, the solution was overlaid with mineral oil and incubated at 50°C overnight. Next, 1 ml of clean-up resin (Promega Corp., Madison, WI, USA) was added to the lower layer, and the resulting solution was mixed in an upturned position and then injected into a column. After rinsing with 2 µl of 80% isopropanol, the column was centrifuged at 15,000 rpm for 3 min to remove isopropanol completely, after which 50 µl of distilled water (70°C) was added directly to the column, and the column was centrifuged at 15,000 rpm for 2 min to extract DNA adsorbed on the column. Then, 5.5 µl of 2 N NaOH was added to the resulting DNA solution, and after mixing the solution was incubated at 37°C for 20 min, after which 66 µl of 5 N ammonium acetate and 243 µl of 95% ethanol were added. The solution was then incubated at -80°C for 1 h and centrifuged at 15,000 rpm for 30 min to precipitate DNA. Approximately, 50 µl of the supernatant was left in the tube, and the rest of the supernatant was collected, mixed with 1 ml of 70% ethanol, and then centrifuged at 15,000 rpm for 30 min to rinse

the DNA. The precipitated DNA was air-dried and dissolved in 20 µl of distilled water; 2 µl of this solution was used as the MSP template solution. AmpliTaq Gold and 10X PCR buffer/MgCl₂ with dNTP (Applied Biosystems, Foster City, CA, USA) was used in the PCR analysis, and DNA was analyzed using a GeneAmp PCR System 9700 (Applied Biosystems). The PCR conditions for other genes and primer sequences are shown in Table I. DNA extracted from the culture cell lines was also used in MSP analysis of *CHFR*.

Statistical analysis. Correlations of aberrant DNA hypermethylation of *CHFR* with the grade of histological differentiation and the cancer stage at surgery were analyzed using the χ^2 test and Mann-Whitney test, respectively. Correlation of aberrant DNA hypermethylation of *CHFR* with patient age was also examined, after establishing that the groups of patients with and without aberrant hypermethylation had a normal age distribution. The Mann-Whitney test was used to examine whether the population medians of the two independent groups differed significantly.

RNA extraction and expression analysis of *CHFR* using RT-PCR. Total-RNA was extracted from 6 endometrial cancer-derived cell lines using a RNeasy mini-Kit (Qiagen, Valencia, CA, USA). cDNA was synthesized with 1 µg of total-RNA using a SuperScript II Reverse Transcriptase kit (Invitrogen, Carlsbad, CA, USA). Synthesized 1st strand cDNA (1 µl) was used as a template solution in RT-PCR analysis of *CHFR* expression. AmpliTaq Gold and 10X PCR buffer/MgCl₂ with dNTP (Applied Biosystems) was used in the PCR analysis, and DNA was analyzed using a GeneAmp PCR System 9700 (Applied Biosystems). The PCR conditions and primer sequences are shown in Table I.

Demethylation. SNG-II cells, which are endometrial cancer-derived cells with aberrant hypermethylation of *CHFR*, were plated on a 10-cm dish at 10⁶ cells/dish and incubated for 72 h. A demethylating agent, 5-aza-dC (Sigma), was then added until its final concentration in the culture medium was 1 µM. Forty-eight hours after the first addition 5-aza-dC was added again, and DNA and RNA were extracted 24 and 72 h after the second addition, respectively.

Cell cycle analysis using flow cytometry. SNG-II and KLE cells, which are both endometrial cancer-derived cell lines, were plated on a 10-cm dish at 5x10⁵ cell/dish and incubated

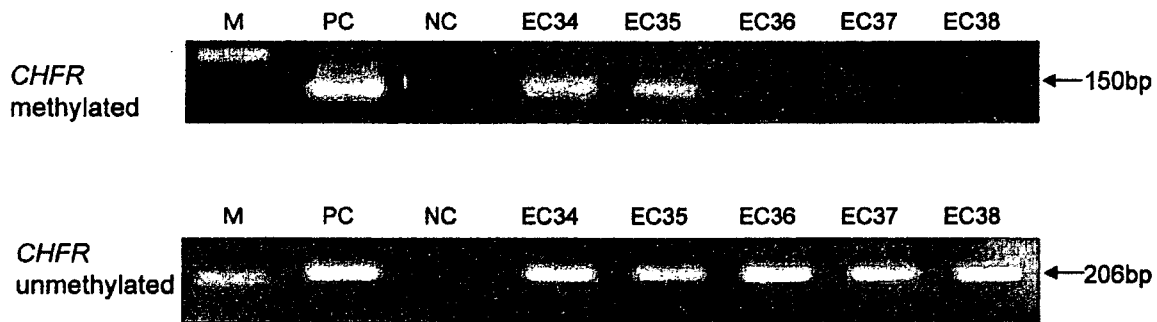


Figure 1. MSP analysis of *CHFR* in endometrial cancer cells obtained using cytology. MSP analysis was conducted with DNA extracted from specimens of endometrial cancer. Bands due to aberrant hypermethylation are found in lanes EC34 and EC35. M, marker; PC, positive control; NC, negative control; EC, endometrial cancer.

to 80% confluence. Paclitaxel (Bristol-Myers Squibb Co., NY, USA) was then added until its final concentration in the culture medium was 1.0 $\mu\text{g/ml}$. Forty-eight hours later, the cells were treated with trypsin, washed twice with PBS, and then centrifuged at 15,000 rpm for 5 min. The supernatant was removed and the cell pellet was washed with 500 μl of PBS. The vortexed cells were combined with 1 ml of 100% cold ethanol and then incubated at room temperature for 30 min for fixation. After rinsing twice with PBS and removing the supernatant, 500 μl of RNase was added to the cell pellet and the mixture was incubated at room temperature for 20 min. After a further addition of 500 μl of propidium iodide (PI), the cells were strained with a cell strainer and cell cycle status was determined using an EpicsXL MCL flow cytometer (Beckman Coulter Inc., Fullerton, CA, USA).

Anticancer drug-sensitivity test. A collagen gel droplet-embedded culture drug-sensitivity test (CD-DST) was performed using 6 endometrial cancer-derived cell lines and 12 of 50 specimens of endometrial cancer (6). The culture cells and specimens were treated with a cell-dispersing enzyme, EZ (Nitta Gelatin Inc., Tokyo, Japan), for 2 h and centrifuged. The cells were preincubated in a collagen gel flask for 24 h and the living cells that attached to the collagen gel were collected. Cellmatrix Type CD solution was added to these cells, and then 3 drops of a 30- μl /drop collagen gel cell suspension were placed in a 6-well plate. The cell suspension was left to stand for 1 h in an incubator under 5% CO_2 at 37°C, and after gelation the medium was doubled to 4 ml/well and anticancer drugs were added. Four anticancer drugs, cisplatin, doxorubicin, paclitaxel and docetaxel, were used at final concentrations of 2.0, 0.02, 1.0 and 0.1 $\mu\text{g/ml}$, respectively. Twenty-four hours after drug administration, the cells were washed to remove the anticancer drugs and then incubated without serum for 7 days under 5% CO_2 at 37°C. After staining with Neutral Red, the cells were fixed with formalin and dried, and cell images were processed using an image analyzer. In the CD-DST, drug sensitivity is assessed using the ratio (T/C) of the number of living cells cultured in a solution containing anticancer drug (T) to that of control cells cultured in a solution without anticancer drug (C).

Expression analysis of *CHFR* protein. Specimens of endometrial cancer (G3) from 4 patients with aberrant hypermethylation of *CHFR* were embedded with OCT compound and

fixed in liquid nitrogen. Cryostat-sliced sections were applied to slides and fixed with 100% ethanol, and the slides were incubated at 4°C overnight with primary antibody (anti-*CHFR* antibody; Santa Cruz, Delaware, CA, USA) diluted 100-fold with 1% BSA in PBS. After rinsing three times with PBS, the slides were incubated with secondary antibody (biotin-labeled anti-goat IgG) at room temperature for 30 min, and after three further rinses with PBS the slides were incubated with ABC (avidin-biotin peroxidase) complex at room temperature for 30 min. After further rinsing three times with PBS, the slides were treated with 0.2 mg/ml diaminobenzidine (DAB) for about 5 min as a color reaction. After rinsing twice with PBS, the slides were treated with hematoxylin solution for nuclear staining, then dehydrated and enclosed, and observed microscopically. Immunohistochemical data for staining of *CHFR* protein were assessed using the following criteria: specimens with 30% or more of stained tumor cells were considered positive, and specimens with <30% of tumor cells showing staining were considered negative.

Results

Partial results of MSP analysis of endometrial cancer cells obtained using liquid-based cytology are shown in Fig. 1. Endometrial cancer specimens had a 12.0% (6/50) frequency of aberrant hypermethylation of the promoter region of *CHFR*, whereas specimens of atypical endometrial hyperplasia and normal endometrial cells in the proliferative and secretory phases showed no aberrant hypermethylation of the *CHFR* promoter region (Fig. 1, Tables II and III).

Correlations of aberrant DNA hypermethylation of the *CHFR* promoter with clinicopathological factors were examined in endometrial cancer patients. The frequency of aberrant hypermethylation in G3 adenocarcinoma was significantly higher than in G1 adenocarcinoma ($p < 0.05$). Aberrant DNA hypermethylation is also generally thought to increase with age, but no significant difference in mean age was found between patients with and without aberrant hypermethylation of *CHFR*. Therefore, these data do not indicate that aberrant hypermethylation occurs more frequently in elderly patients with endometrial cancer (Table IV).

Of the 6 culture cell lines derived from endometrial cancer, SNG-II and HEC108 cells showed aberrant hypermethylation

Table II. Frequency of aberrant DNA hypermethylation of *CHFR* in specimens of endometrial cancer.

No.	Age	Tissue type	Stage	Differentiation	<i>CHFR</i>
EC1	52	EM	Ib	G3	U
EC2	50	EM	Ia	G1	U
EC3	51	EM	IIIc	G1	U
EC4	54	AS	IIIc	G3	M
EC5	51	EM	Ia	G1	U
EC6	61	EM	Ib	G1	U
EC7	70	EM	IIIc	G2	U
EC8	61	EM	IIb	G1	U
EC9	62	AS	IIIa	G2	U
EC10	40	EM	IIa	G1	U
EC11	59	EM	IIa	G3	U
EC12	57	EM	Ib	G3	U
EC13	80	EM	IIIc	G3	U
EC14	54	AS	Ib	G1	U
EC15	53	EM	Ib	G3	U
EC16	42	EM	IIb	G1	U
EC17	71	EM	IIIc	G3	U
EC18	60	EM	Ib	G1	U
EC19	57	EM	IIIa	G2	U
EC20	71	EM	IIa	G1	U
EC21	37	EM	IIa	G2	U
EC22	47	EM	IIIb	G1	U
EC23	67	EM	Ic	G2	M
EC24	53	EM	Ia	G1	U
EC25	69	EM	IIIc	G2	U
EC26	55	EM	IIIc	G2	U
EC27	54	EM	Ia	G1	U
EC28	63	EM	Ia	G1	U
EC29	41	EM	Ib	G1	U
EC30	62	AS	Ib	G1	U
EC31	58	EM	Ib	G2	U
EC32	56	EM	IIIc	G3	M
EC33	71	EM	Ib	G2	U
EC34	53	AS	Ib	G3	M
EC35	50	EM	IIIa	G3	M
EC36	42	AS	IIIc	G3	U
EC37	55	EM	Ic	G3	U
EC38	34	AS	IIIc	G1	U
EC39	61	EM	Ic	G1	U
EC40	61	EM	Ic	G1	U
EC41	61	EM	Ib	G1	U
EC42	59	EM	Ib	G1	U
EC43	55	AS	IVb	G2	U
EC44	54	EM	IIa	G1	U
EC45	78	EM	Ib	G3	U
EC46	65	EM	Ib	G2	M
EC47	68	EM	IIIc	G3	U
EM48	54	EM	IIIc	G2	U
EM49	60	EM	Ib	G1	U
EC50	70	EM	IVb	G2	U

EC, endometrial cancer; EM, endometrioid adenocarcinoma; AS, adenosquamous carcinoma; G1, well-differentiated; G2, moderately differentiated; G3, poorly differentiated; M, methylated; U, unmethylated.

Table III. Frequency of aberrant DNA hypermethylation of *CHFR* in cells of normal endometrium and atypical endometrial hyperplasia.

No.	Age	Tissue type	<i>CHFR</i>
AE1	30	AEH	U
AE2	32	AEH	U
AE3	35	AEH	U
AE4	35	AEH	U
AE5	46	AEH	U
AE6	41	AEH	U
AE7	50	AEH	U
AE8	45	AEH	U
AE9	47	AEH	U
AE10	45	AEH	U
NE1	51	Sec	U
NE2	52	Sec	U
NE3	44	Sec	U
NE4	23	Sec	U
NE5	34	Sec	U
NE6	43	Pro	U
NE7	42	Pro	U
NE8	44	Pro	U
NE9	32	Pro	U

AE, atypical endometrial hyperplasia; NE, normal endometrium; AEH, atypical endometrial hyperplasia; Sec, secretory phase; Pro, proliferative phase; U, unmethylated.

Table IV. Correlation of aberrant DNA hypermethylation of *CHFR* with histological differentiation, stage at surgery and mean onset age.

	<i>CHFR</i>		P-value
	Methylated	Unmethylated	
G1	0	23	<0.05
G2	2	11	
G3	4	10	
Stage			NS
I	3	22	
II	0	7	
III	3	13	
IV	0	2	
Mean onset age	57.5±6.90	57.4±10.34	NS

G1, well-differentiated; G2, moderately differentiated; G3, poorly differentiated.

of *CHFR*, and RT-PCR analysis of *CHFR* expression showed reduced mRNA levels in these cells (Fig. 2). Consistent with this observation, the SNG-II and HEC108 cells showed higher

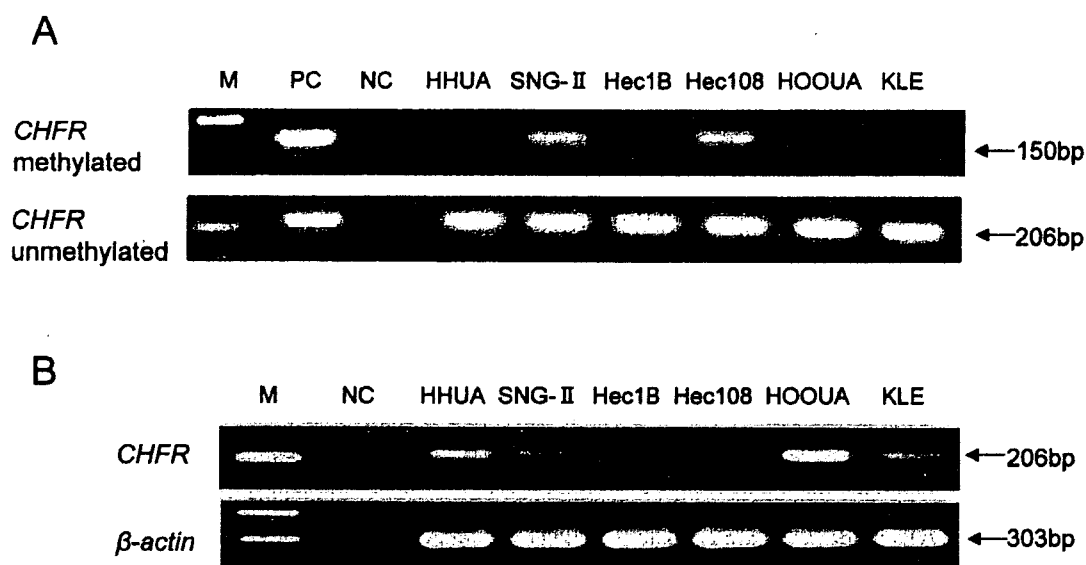


Figure 2. (A), MSP analysis of *CHFR* in endometrial cancer-derived cell lines. Aberrant hypermethylation of *CHFR* was found in two cell lines, SNG-II and HEC108. (B), Expression analysis of *CHFR* in endometrial cancer-derived cell lines using RT-PCR. *CHFR* expression was reduced in SNG-II and HEC108 cells, which showed aberrant hypermethylation of *CHFR*. M, marker; PC, positive control; NC, negative control.

Table V. Sensitivity (T/C ratio) of endometrial cancer-driven cells to various anticancer drugs in the CD-DST.

Cell line	<i>CHFR</i>	Cisplatin (%)	Doxorubicin (%)	Paclitaxel (%)	Docetaxel (%)
HHUA	U	100	100	22.5	31.0
SNG-II	M	52.0	65.1	16.7	15.1
Hec1B	U	91.1	85.7	71.2	65.9
Hec108	M	56.6	76.6	11.8	20.6
HOOUA	U	94.2	88.4	20.7	50.9
KLE	U	57.6	93.6	60.8	63.9

M, methylated; U, unmethylated.

sensitivity to paclitaxel and docetaxel in the CD-DST, compared to that of other cell lines (Table V).

Following treatment of SNG-II cells with 5-aza-dC, the aberrant hypermethylation band in the MSP analysis was weaker than that before administration of 5-aza-dC, and recovery of *CHFR* expression was shown in these cells (Fig. 3). Differences in sensitivity of SNG-II and HEC108 cells, and of KLE cells (which do not show aberrant hypermethylation of *CHFR*), to four anticancer drugs were examined using the CD-DST before and after 5-aza-dC administration. The T/C ratios of cells treated with cisplatin and doxorubicin did not differ before and after 5-aza-dC administration, regardless of the presence or absence of aberrant hypermethylation of *CHFR*, showing that 5-aza-dC administration had no effect on sensitivity to cisplatin and doxorubicin. Similarly, the T/C ratios of KLE cells treated with paclitaxel and docetaxel were unchanged by 5-aza-dC administration. However, the T/C ratios in SNG-II and HEC108 cells treated with paclitaxel and docetaxel significantly increased after 5-aza-dC administration, showing that these cells initially had low sensitivity to taxanes (Table VI).

Cell cycle changes in SNG-II and KLE cells treated with paclitaxel alone or combined paclitaxel and 5-aza-dC were determined using flow cytometry. The percentages of paclitaxel-treated KLE cells in the G2/M and Sub-G1 phases were 67.3 and 5.1%, respectively; these data were almost the same as those for untreated control cells. KLE cells treated with paclitaxel and 5-aza-dC gave similar results. In contrast, the percentage of paclitaxel-treated SNG-II cells in the G2/M phase was very low (0.2%) and the percentage of these cells in the Sub-G1 phase was higher (13.3%) compared to control cells, indicating that paclitaxel administration induced apoptosis. However, with combined paclitaxel and 5-aza-dC treatment, the percentage of SNG-II cells in the G2/M phase was high (82.7%) and that for cells in the Sub-G1 phase was low (1.8%) compared to control cells; a similar pattern to that seen for paclitaxel-treated KLE cells (Fig. 4).

MSP analysis indicated aberrant hypermethylation of *CHFR* in 12.0% (6/50) of endometrial cancer specimens, with this being particularly common for G3 specimens (4/14, 28.6%). Immunohistochemical analysis was conducted on specimens showing aberrant hypermethylation of *CHFR* from